Chlorine peroxide reaction explains observed wintertime hydrogen chloride in the Antarctic vortex

communications earth & environment

Article

A Nature Portfolio journal

https://doi.org/10.1038/s43247-025-02499-4

Chlorine peroxide reaction explains observed wintertime hydrogen chloride in the Antarctic vortex

Jens-Uwe Grooß [1] ✉, Rolf Müller [1], John N. Crowley [2] & Michaela I. Hegglin [1,3,4]

It is well established that the drastic ozone loss in the Antarctic stratosphere, commonly known as the ozone hole, is primarily driven by gas-phase and heterogeneous chemical processes. While chemistry transport models generally reproduce observed ozone depletion well, they fail to capture the rapid early-winter decline of hydrogen chloride. We here examine the impact of the heterogeneous reaction between chlorine peroxide and hydrogen chloride forming HOOCl, followed by its photolysis. Incorporating this reaction and an additional hypochlorous acid loss pathway into a chemical mechanism significantly improves model agreement with observed levels of several chlorine compounds in the lower polar vortex stratosphere. This revised mechanism increases simulated ozone partial column depletion by over 15% between early July and mid-September 2011. Laboratory confirmation of these proposed reactions is needed to validate the mechanism.

The discovery of extensive, lower stratospheric ozone depletion in the Antarctic spring, commonly known as the ozone hole[1,2], came as a complete surprise although chlorine-catalysed ozone depletion in the mid-stratosphere had been discussed before[3]. Nevertheless, after its discovery, the main processes leading to the formation of the ozone hole were rapidly established[4–7] and current models reproduce the rapid depletion of ozone in the Antarctic spring[8].

However, model simulations do not fully reproduce the temporal evolution of the relevant chemical compounds both in latitude and altitude. In particular, discrepancies between observations and simulations of chlorine compounds in the polar stratosphere have been found[9–12]. This discrepancy in hydrogen chloride has been consistently reported across four independent models[11,12], suggesting a systematic issue. At the onset of the Polar Stratospheric Cloud (PSC) period, the heterogeneous reaction between chlorine nitrate ($ClONO_2$) and HCl to form Cl_2 and HNO_3 typically leads to near-complete $ClONO_2$ depletion and a moderate reduction in HCl, as $ClONO_2$ mixing ratios in early winter are typically much smaller than HCl mixing ratios. Both initial depletions are typically well reproduced by models. However, observations indicate a further depletion of HCl to very low values after this step which is not reproduced by state-of-the-art models. Several potential missing processes to explain this discrepancy have been explored. Wohltmann et al. highlighted the HCl discrepancy during early winter and suggested a temperature reduction for calculations of the HCl solubility in the liquid aerosol[11,13]. However, this hypothetical process should cause a removal of gas-phase HCl and a dissolution into the liquid aerosol with decreasing temperatures, which has not been observed, not even for temperatures between 182 K and 186 K[12]. Further hypotheses include N_2 ionisation from galactic cosmic rays, photolysis of particulate HNO_3, and decomposition of particulate HNO_3 by other mechanisms[12]. So far, no convincing explanation for the observed HCl depletion has been found. A detailed analysis suggests that the missing processes are associated with temperatures low enough for heterogeneous chlorine activation on PSCs or cold aerosols, as well as available sunlight[12].

Here, we investigate a process involving chlorine peroxide (Cl_2O_2) and HOOCl that thus far has not been implemented in global simulations. This process has been considered only in a few simple chemical box model simulations[14] based on laboratory studies conducted on halide ice surfaces[15]. The potential role of HOOCl in stratospheric chemistry was discussed by Warneck[16], but was largely ignored in subsequent studies. In the early winter vortex, after the heterogeneous reaction between HCl and $ClONO_2$ has completely depleted $ClONO_2$, the available active chlorine in the form of ClO or Cl_2O_2 may interact with the PSCs. We therefore have investigated the impact of the heterogeneous reaction

$$Cl_2O_2 + HCl \rightarrow HOOCl + Cl_2 \qquad \text{(R1)}$$

which has been previously proposed based on laboratory measurements of this reaction on ice surfaces[14,15].

[1]Institute of Climate and Energy Systems – Stratosphere (ICE-4), Forschungszentrum Jülich, Jülich, Germany. [2]Division of Atmospheric Chemistry, Max-Planck-Institute for Chemistry, Mainz, Germany. [3]Institute for Atmospheric and Environmental Research, University of Wuppertal, Wuppertal, Germany. [4]Department of Meteorology, University of Reading, Reading, UK. ✉e-mail: j.-u.grooss@fz-juelich.de

The HOOCl product may be photolysed to form OH + ClO

$$HOOCl + h\nu \rightarrow OH + ClO \quad (R2)$$

Besides its photolysis, the direct decomposition of HOOCl into HCl+O_2 is also discussed which would not have any net effect on HCl[14]. This competitive effect would reduce the effective photolysis rate. We do not pursue this further here as the photolysis rate itself is not known.

Our simulations with heterogeneous reaction R1 and the photolysis reaction R2 resulted in substantial increases in model hypochlorous acid (HOCl) as a result of the reaction HO_2 + ClO. Especially for near zero HCl mixing ratios in the dark polar stratosphere, the heterogeneous reaction with HCl cannot further deplete HOCl which contrasts with observations shown below. Therefore an additional HOCl sink (its self-reaction)

$$HOCl + HOCl \rightarrow \text{products} \quad (R3)$$

was incorporated as a gas-phase reaction in the model with the products H_2O and Cl_2O. This reaction would reduce HOCl mixing ratios also in the polar night. Cl_2O is decomposed to Cl and ClO in the model.

The reference simulation which represents the state-of-the art Antarctic polar chemistry scheme and uses a very similar model setup as our previous study[12] is labelled as CLaMS Ref. The simulation uses currently recommended reaction kinetics[17]. The simulation that additionally includes reactions R1 and R2 is labelled CLaMS A and the simulation that includes reactions R1, R2 and R3 is labelled CLaMS B. As these reactions have not been characterised in laboratory experiments, we make the following assumptions: The heterogeneous reaction R1 was considered here only on liquid aerosol and its reaction probability was set to be identical to that of the reaction $ClONO_2$+HCl with a temperature-dependent uptake coefficient calculated from the solubility of HCl in the liquid aerosol[18,19]. This choice is somewhat arbitrary, but potentially the exact number may be not critical, as often the heterogeneous reactions are not rate limiting in reaction chains.

HOOCl has been detected in laboratory experiments by IR spectroscopy and its photolysis has been reported for UV light of wavelengths between 365 nm and 405 nm[20]. As the absorption cross sections of HOOCl are unknown, we assume a photolysis frequency identical to that of HOCl as also suggested by DeHaan et al.[14]. The rate constant for reaction R3 has also not been measured to our knowledge, but quantum chemical calculations[21] suggest reaction rate constants for the products ClO + Cl + H_2O and for the products Cl_2O + H_2O for temperatures ≥300 K. Here we assume an additional reaction R3 with the products ClO + Cl + H_2O (assuming immediate decomposition of Cl_2O to ClO + Cl) and the reaction rate constant of $3 \cdot 10^{-15}$ cm^3s^{-1}. This number is below the 300 K value from theoretical calculations[21] ($4.8 \cdot 10^{-15}$ cm^3s^{-1}), but above the value extrapolated to 200 K ($1.4 \cdot 10^{-15}$ cm^3s^{-1}). Sensitivity simulations with respect to the choice of these kinetic parameters are shown in Figures S1 to S5 of the supplementary information. In our simulation the HOOCl mixing ratios reach the order of 1 ppb(v for the times in early winter when HCl mixing ratios deplete to almost zero. Otherwise HOOCl is typically well below 0.1 ppbv.

Results

With the above described chemistry setups Ref, A, and B, global CLaMS simulations were performed for the period from May to October 2011, a time period for which MLS, MIPAS, and ACE-FTS observations were available. In addition to these simulations, we also show a chemical box model simulation over this period that best represents the mean development of chlorine compounds in the vortex core at altitudes of the greatest HCl discrepancy. Using the box model, one can not only document the changes induced by chemistry, but also investigate the sensitivity with respect to the kinetic parameters at low numerical cost (compare supplementary information). For that purpose, about 8200 air parcel trajectories were calculated starting between 550 and 600 K potential temperature within the polar vortex core (defined as equivalent latitude[22] south of Φ_e = 75°S). Along those trajectories, CLaMS chemistry was simulated and then one example trajectory was chosen in which the development of HCl, $ClONO_2$, and HOCl along the trajectory is closest to the mean of the global model simulation. The air parcel described by this example trajectory starts at 550 K and descends down to about 435 K potential temperature in early September. The box-model results for the simulations CLaMS Ref, A and B along this trajectory are shown in Fig. 1. The HCl depletion in the simulations CLaMS A and B continues in early June unlike in CLaMS Ref. It is also evident that in simulation A, HOCl acts as a temporary chlorine reservoir instead of HCl in June to August. In simulation B, HOCl mixing ratios are reduced by the HOCl self reaction R3 with the consequence of increased active chlorine and a somewhat earlier onset of ozone depletion.

Development of hydrogen chloride in polar stratospheric winter

In Fig. 2, the 3-dimensional model simulations of HCl as well as the observations are shown averaged in the coordinate system of equivalent

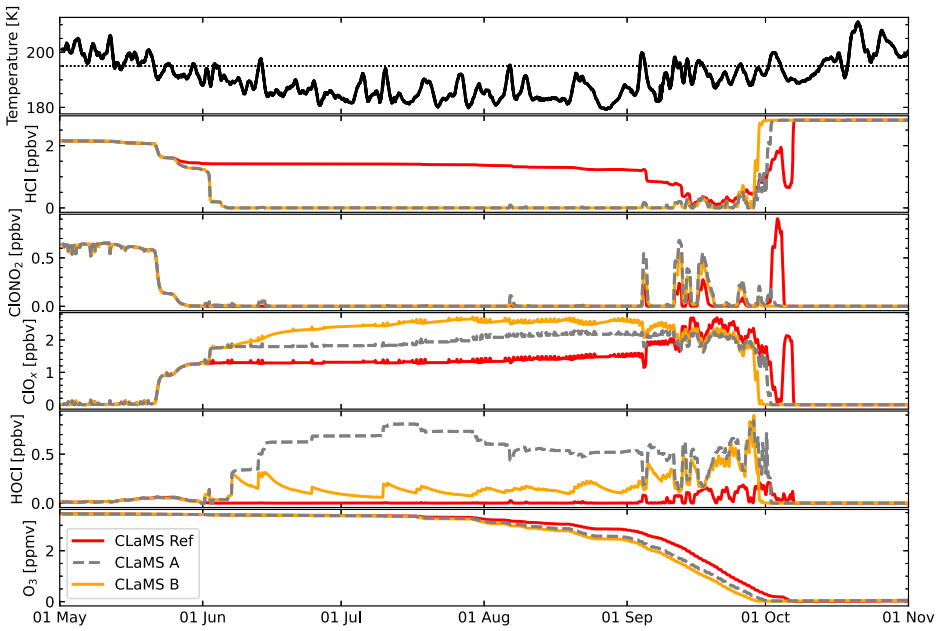

Fig. 1 | Box model results along an example trajectory highlighting the impact of the proposed chemical mechanism. Shown are the trajectory temperature and simulated mixing ratios of HCl, $ClONO_2$, ClO_x (=ClO + 2Cl_2O_2 + 2Cl_2), HOCl, and O_3 for the different suggested chemical mechanisms from the CLaMS simulations Ref (red), A (grey dashed), and B (orange). In the top panel, the temperature 195 K is indicated as a dotted line representing the typical threshold of the onset of heterogeneous chemistry.

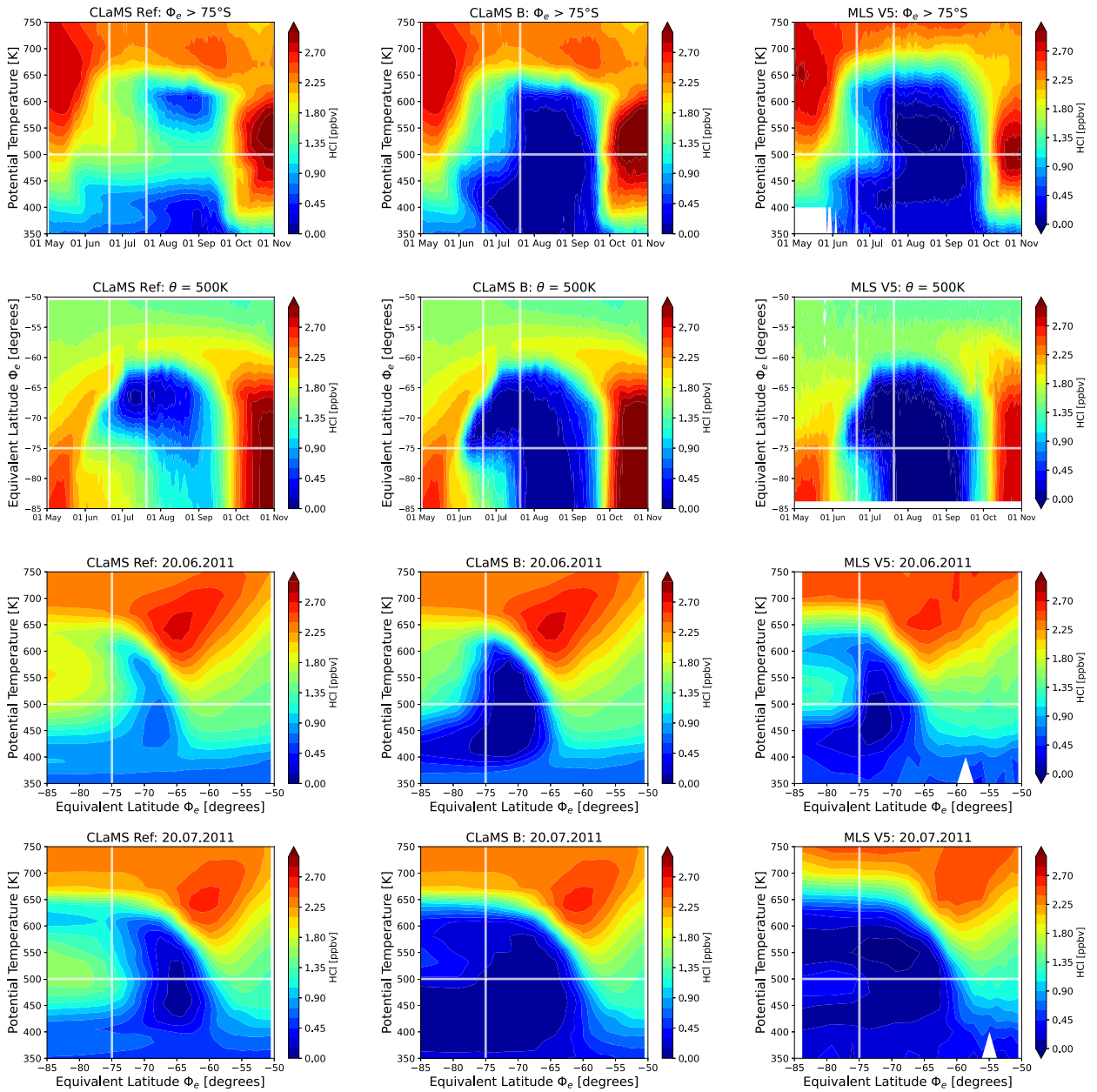

Fig. 2 | Comparison of the development of HCl observed by MLS and simulated by CLaMS. HCl mixing ratios are averaged in equivalent latitude/potential temperature bins. The left panel column shows CLaMS results for May to November 2011 from the reference simulation Ref, the middle panel column shows the corresponding simulations B with the added reactions R1-R3. The right panel column shows the corresponding MLS observations. The top panel row shows the vortex-core average for equivalent latitudes pole-ward of 75°S as a function of time and potential temperature. The middle panel row shows the time development on the 500 K potential temperature level. The bottom two panel rows show snapshots of this average for 20 June and 20 July 2011, respectively. White lines on the panels indicate the cuts or borders displayed in the other panels of this figure.

latitude Φ_e and potential temperature. The figure shows HCl mixing ratio in various slices as a function of equivalent latitude Φ_e, potential temperature θ and time, both for the MLS observations and for the simulations Ref and B. This figure illustrates the details of the temporal evolution of the HCl mixing ratios both in latitude and altitude over the entire simulation period. It is evident that the HCl mixing ratio over the vortex lifetime and especially the evolution of HCl mixing ratios in the vortex core at the 500 K level is reproduced much better by simulation B with the reactions R1, R2 and R3 included. Figure 3a shows the vortex core average of the HCl observations and simulations on the 500 K level. The simulations A and B are able to reproduce the HCl depletion steps from June to August in contrast to CLaMS Ref. The HCl variability within the vortex core at this level, represented by the range of one standard deviation of the model results within an equivalent latitude-potential temperature bin, is also comparable with the corresponding range encompassed by the standard deviation of observations (see also Figure S4a in the supplementary information).

The chlorine deactivation in late September and early October takes place about one week too early in CLaMS A and B. This is likely due to somewhat lower simulated ozone mixing ratios than observed, as especially the low ozone mixing ratios trigger the chlorine deactivation into HCl[23]. This also causes deviations in other chlorine species which is however not in the focus of this study.

Chlorine nitrate

As the largest discrepancy between observed and simulated HCl in Fig. 2 occurs around 500 K potential temperature, we compared the time

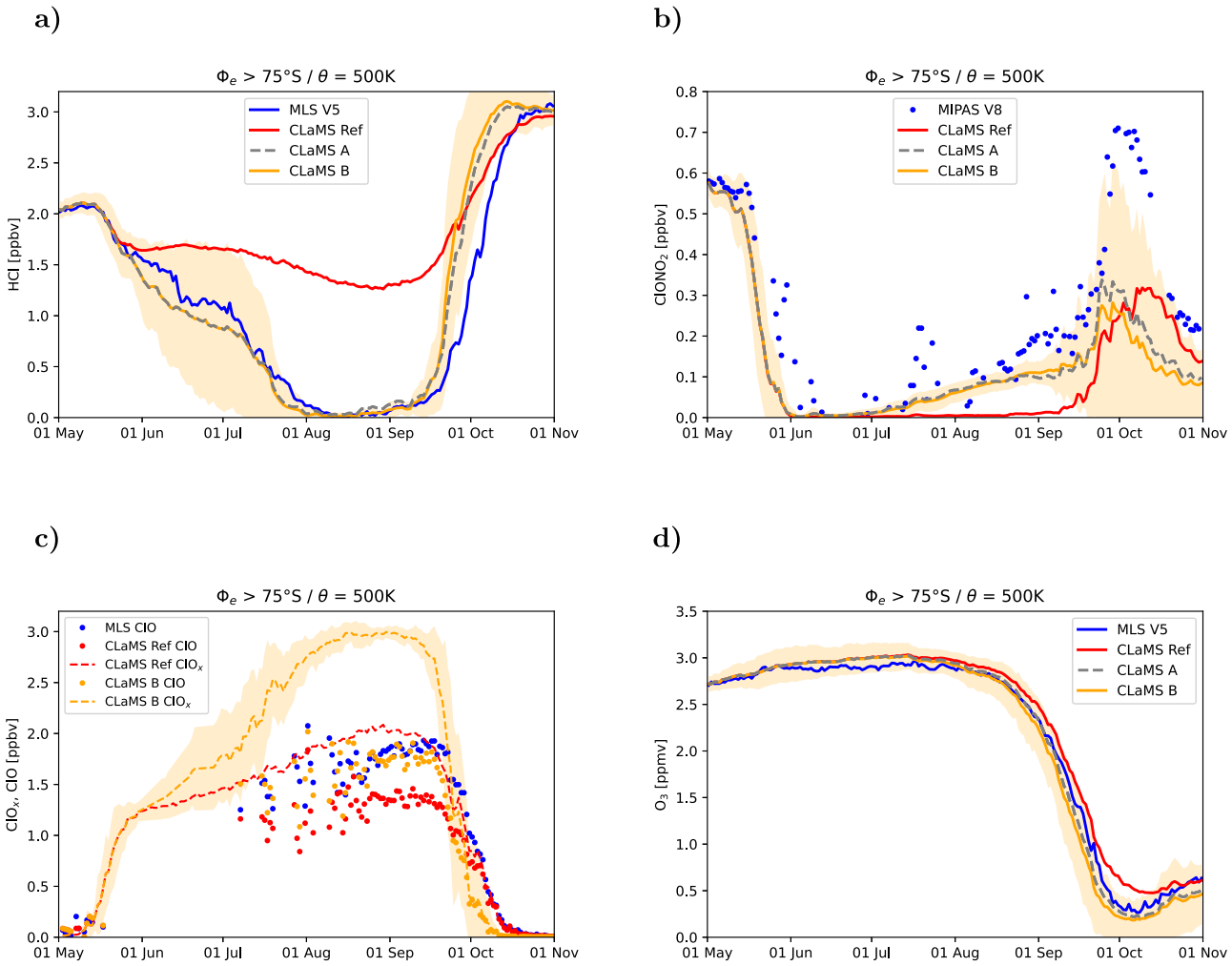

Fig. 3 | Vortex core average model results and corresponding observations. Shown are mean mixing ratios in the vortex core (Φ_e > 75°S) on the 500 K isentrope for HCl, $ClONO_2$, ClO and O_3 for the different model settings. Observations of MLS and MIPAS are shown as blue lines or symbols. The red line and symbols correspond to the reference simulations CLaMS Ref. CLaMS simulations A and B are shown with grey dashed lines and orange colors, respectively. The orange shaded region shows the ± 1 standard deviation range of simulation B. Panel **a** shows HCl and panel **b** shows $ClONO_2$. In panel **c**, colored dots show the average is over ClO observations with solar zenith angle below 92° and corresponding simulations for the same times and locations. The dashed lines show CLaMS ClO_x (= ClO + 2 Cl_2O_2 + 2 Cl_2). For the sake of clarity, not all available simulations are shown in all panels. Panel **d** shows the corresponding ozone mixing ratios from MLS observations and the CLaMS simulations.

evolution of vortex core average mixing ratios of chlorine nitrate ($ClONO_2$) at this level with observations by MIPAS (see Fig. 3b). The initial decrease in HCl in May due to the reaction $ClONO_2$+HCl is captured by all simulations. However, the continued depletion steps of HCl from late May through August are only reproduced in simulations A and B. MIPAS data also indicate a steady $ClONO_2$ increase from June to September. This increase in $ClONO_2$ is not present in the reference simulation, but is better reproduced for the simulations A and B. In the box model simulation in Fig. 1, $ClONO_2$ mixing ratios remain near zero throughout the polar winter except for occasional increases in both HCl and $ClONO_2$ during September. These increases correspond to intermediate temperature rises, which temporarily reduce the heterogeneous reaction rate for HCl+$ClONO_2$, allowing both species to increase briefly. The $ClONO_2$ increase is shown in Fig. 3b. In September and October, the large variability of $ClONO_2$ is also visible in the standard deviation of the model results. None of the simulations is able to reproduce the magnitude of the observed average $ClONO_2$ increase in early October. The difference reaches about one standard deviation of the model results. It is important to note that MIPAS observations are typically unavailable within PSCs. This likely biases the MIPAS averages high, as the data reflect predominantly regions with higher temperatures and consequently higher $ClONO_2$ levels compared to the simulations.

Chlorine monoxide

A comparison of the simulations with chlorine monoxide (ClO) observations is complicated by the ClO diurnal cycle with maximum values typically around local noon and near zero values during night. For the comparison presented here, the CLaMS chemistry was thus calculated along trajectories ending at the time and location of individual MLS observations. In Fig. 3c, we show that the simulations with the new mechanism show much better agreement with observed ClO especially throughout August and September. Figure 3c also shows the simulated active chlorine ClO_x (=ClO +2Cl_2O_2+2Cl_2) from the model versions as dashed lines. As there are no direct available observations of ClO_x, the good agreement between ClO observations with CLaMS B implies that the much higher levels of active chlorine in CLaMS B are more realistic than those in Ref.

Hypochlorous acid

A comparison of the model results with hypochlorous acid (HOCl) observations from ACE-FTS shows the effect of the postulated HOCl self-reaction R3 most clearly. Because of the sparse geographical coverage of ACE-FTS, the CLaMS results were interpolated to the satellite's observation locations. In Fig. 4, daily HOCl mixing ratios averaged within the vortex core are shown as well as the corresponding model results. If more than one

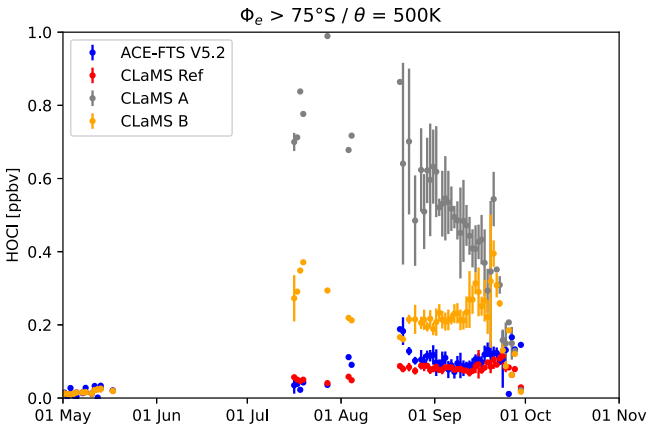

Fig. 4 | Vortex core HOCl comparison. Similar to Fig. 3, HOCl observations by ACE-FTS are shown. The corresponding CLaMS results are evaluated at the ACE-FTS observation points. The circles show the diurnal average within the given equivalent latitude range. Vertical bars show the standard deviation of the daily observations. Between late-May and mid-July, there are no observations within the given equivalent latitude range. The measurement accuracy of ACE-FTS in this altitude is about 0.1 ppbv[24].

observation per day is available, the vertical bar shows the standard deviation from all diurnal observations.

As seen in Fig. 4, CLaMS A significantly overestimates the ACE-FTS HOCl mixing ratios. By including the HOCl self reaction, CLaMS B reproduces better the elevated HOCl observations in the polar winter stratosphere, for example from early July to late August in the vortex edge region (not shown). When ACE-FTS observations return to high equivalent latitudes, there are about 200 ppbv on 20 and 21 August, approximately reproduced by simulation CLaMS B. Afterwards the simulation CLaMS B overestimates HOCl suggesting an underestimation in the HOCl sink. This could be improved by a slower reaction R1 (see Figure S5 in the supplementary information), but this is not in the focus of this study. The reference simulation Ref does not show significantly elevated HOCl values since HOCl would immediately react heterogeneously with the still available HCl. Generally, observations of elevated HOCl mixing ratios in the winter polar vortex have been published both by ACE-FTS and MIPAS[24,25]. ACE-FTS reports large HOCl mixing ratios in the Antarctic lower stratosphere with maximum values even on the order of 500 pptv[24]. A climatology of HOCl from the early phase of Envisat-MIPAS, when the instrument operated with higher spectral resolution, also shows elevated HOCl levels in the polar stratosphere[25]. The proposed mechanism would therefore possibly also help to explain the polar stratospheric HOCl observations.

Ozone depletion

The box model simulation (Fig. 1) indicates that the incorporation of the new reactions R1, R2, and R3 results in additional ozone depletion, however, this effect is not large due to the low amount of available sunlight in mid-winter in the polar vortex core. As expected for the Antarctic[8,23], ozone is nearly completely depleted by spring, with the simulations A and B reaching minimum ozone mixing ratios about one week earlier than in the reference simulation because of the enhanced chlorine activation.

The observed ozone development at the 500 K level, shown in Fig. 3d, is generally well reproduced in the global 3-dimensional simulations, potentially with a slight over-estimation of ozone depletion. The minimum of the average vortex core ozone in simulations A and B at this level is about 0.4 ppm smaller than in the reference simulation and compares better with the MLS observations, likely because of a better simulation of active chlorine.

To investigate the effect of the proposed chemistry across the full depth of the polar vortex we also calculate depletion in a partial ozone column. Figure 5 presents the simulated ozone depletion between 380 K and 550 K potential temperature both for the vortex core (Φ_e > 75°S) and the entire vortex(Φ_e > 61°S).

In the vortex core, the maximum partial ozone column depletion in simulation B on 2 October amounts to 185 DU, that is 7.7% more than in the reference simulation and 2.4% more than in simulation A. Because of mixing processes and ongoing ozone depletion in the reference simulation where simulation B reached already near-zero ozone, the difference between the simulations later in October is smaller. When averaging the model results over the entire vortex (Φ_e > 61°S), these effects are reduced. The maximum partial ozone column depletion in simulation B amounts to 169 DU on 12 October, that is 2.9% more than in the reference simulation and 0.4% more than in simulation A. The proposed chemistry of CLaMS B does alter the timing of ozone depletion, with over 15% more ozone column loss in the vortex core between early July and mid September (Fig. 5c). In August and September, the impact of the proposed reactions on simulated ozone loss in CLaMS A is low because of less available active chlorine, due to HOCl being an interim reservoir as explained above. The simulated vortex core partial ozone column for the potential temperature range 380–550 K on 2 October 2011 is reduced from 23.0 DU in CLaMS Ref to 12.2 DU and 8.7 DU for CLaMS A and B, compared to the passive ozone tracer partial column of 195 DU. Thus on this day the partial ozone column is 47% and 62% below the that of CLaMS Ref, respectively (compare Fig. 5e, f). When averaging over the entire vortex area (Φ_e < 61°), the impact of the proposed additional reactions is lower than in the vortex core (compare Fig. 5d, f).

Conclusions

The model simulations reported here demonstrate that the previously reported discrepancy between HCl observations and simulations in the early winter polar vortex in the stratosphere can be resolved by incorporating a heterogeneous reaction of chlorine peroxide with HCl on PSCs with HOOCl as a photo-labile, gas-phase product. Including this reaction and the HOCl self-reaction, simulations of HCl, HOCl, ClO, and $ClONO_2$ are brought much closer to observations than previously possible. The impact of the proposed mechanism on polar ozone loss is moderate as the main differences to simulations with established chemistry schemes occur in the polar night and twilight. However, between early June and mid September, over 15% more column ozone loss is simulated. The simulated remaining partial column ozone on 2 October 2011 including this mechanism is then 62% lower than in the reference simulation in which the maximum ozone column depletion is reached later. These numbers refer to the year 2011 with a stratospheric chlorine loading of slightly over 3 ppbv. Since the signs for the long-term recovery from the ozone hole due to decreasing chlorine levels are currently most evident in September[26], when simulations A and B show a substantial increase in active chlorine (ClO_x) with respect to simulation Ref (Fig. 3c) and the impact on the ozone column is largest (Fig. 3e), the proposed reactions may also be relevant for understanding the recovery of the ozone hole.

Neither the uptake coefficient for the heterogeneous process R1 nor the kinetics of the HOCl self-reaction R3 (either as a gas-phase or a heterogeneous process) have been investigated in detail in laboratory studies. Similarly, absorption cross sections for HOOCl have not been measured and are assumed to be the same as those of HOCl. We conclude that, while the addition of R1 - R3 in model simulations of the evolution of chlorine compounds improves the agreement with observations, laboratory measurements of the proposed heterogeneous and gas-phase reactions are required to strengthen confidence in the chemical scheme put forward here.

Methods

CLaMS model description

We present simulations of the Chemical Lagrangian Model of the Stratosphere (CLaMS). CLaMS is a Lagrangian chemistry-transport model that is described elsewhere[27–29]. Here we use the model setup that was also used previously[12] with updates regarding the initialisation and the most recent recommendations for chemical kinetics[17]. Briefly, the initialisation and the lower and upper boundary are derived from Aura-MLS and Envisat-MIPAS

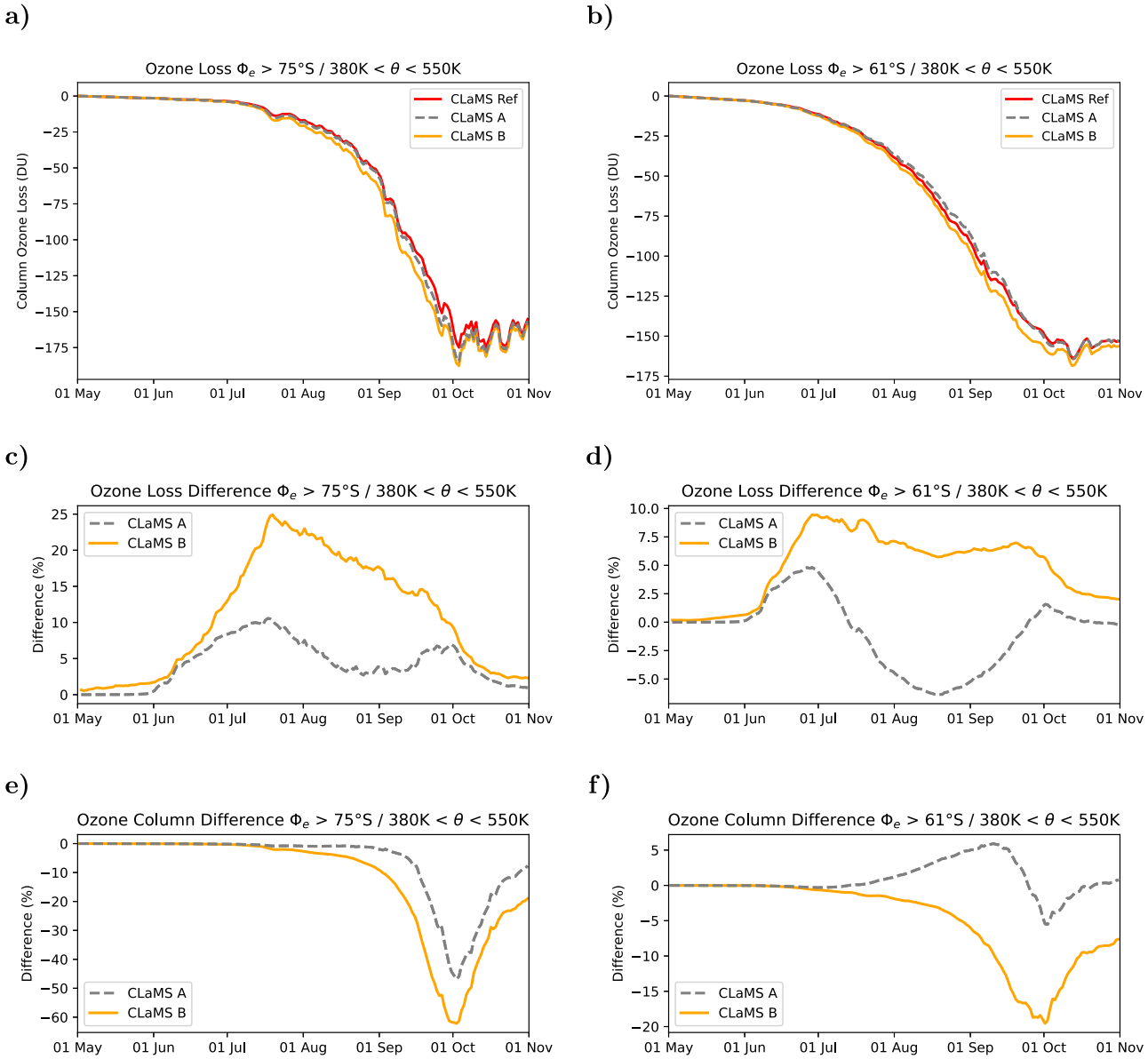

Fig. 5 | Simulated chemical column ozone loss. Shown is the partial ozone column loss (simulated ozone minus passive ozone) between potential temperatures of 380 K and 550 K versus time for equivalent latitudes (**a**) south of 75°S and **b** south of 61°S for the CLaMS simulations Ref, A and B. Panels **c**, **d** show the corresponding percentage difference of the simulations A and B with respect to Ref. Panels **e**, **f** show the corresponding percentage difference of the simulated partial ozone itself.

observations. The global simulation has a horizontal resolution of 100 km south of 40°S and 300 km north of 40°S latitude. The vertical model coordinate is set to hybrid potential temperature ζ, which is equal to potential temperature above about 300 hPa and corresponds to pressure levels below with a smooth transition[30,31]. The simulation has 32 vertical levels from the Earth's surface up to 900 K potential temperature with a vertical resolution of about 900 m in the lower stratosphere. Due to the mixing formulation, the number of Lagrangian air parcels is variable, on average the simulation consists of 435 thousand air parcels. A Lagrangian PSC simulation for NAT and ice is also included[32]. The simulations are for the period from 1 March to 31 October 2011, when MLS, MIPAS and ACE-FTS observations are available. The initialisation of the simulations for all chemical species is identical to that shown previously[12] except for ozone, HCl and $ClONO_2$. Ozone and HCl are initialized here using the MLS version 5 data within ± 2.5 days mapped to the initial time 1 May 2011 12:00 UTC using CLaMS backward and forward trajectories and combined to a grid of 2° latitude and 6° longitude. Similarly MIPAS version 8 $ClONO_2$ data is mapped to the initialisation time. The underlying meteorological wind and temperature data are from ERA5 reanalyses[33] in 1° × 1° horizontal resolution and full vertical resolution with vertical velocities based on heating rates[34].

CLaMS box-chemistry model. As CLaMS is a Lagrangian Model, it is also possible to use it as a box-chemistry model instead of for a global simulation. To do that, the CLaMS trajectory module is used to determine the trajectory from one or more starting points. Using the initial chemical composition for these points, the CLaMS chemistry module calculates the change of chemical composition along individual trajectories. The influence of mixing or boundary emissions cannot be considered in this box model setup. This setup is used here to show a typical development of chemical composition as well as to demonstrate the sensitivity with respect to different assumptions of reaction rate parameters. This model setup was also used to calculate the ClO mixing ratios at the time and location of an individual observation as described in the next section.

CLaMS results at observation locations. The Lagrangian character of CLaMS was used to derive the direct comparison with observations in space

and time. For that, we consider two cases for chemical species with and without substantial diurnal variation due to photo-chemistry, respectively. For slowly varying chemical species, we calculate backward or forward trajectories starting at the observation location and time up to the closest model output time-step, that is 12:00 UTC at the day of observation. Then the model output is interpolated to the trajectory location to obtain the corresponding simulated mixing ratios. For chemical species with substantial diurnal variation like ClO, the chemistry needs to be taken into account. We therefore calculate backward trajectories starting at the observation location and time up to the last model output time-step. The chemical composition is then similarly interpolated to the trajectory location to obtain a box model initialisation. The CLaMS box-chemistry model is then calculated along these trajectories to obtain the corresponding simulated mixing ratios at the observation time.

MLS version 5 data

The HCl observations by the Microwave Limb Sounder (MLS) on board the Aura satellite[35] are the main data set used in this study. MLS observes in limb viewing geometry on the so-called A-train orbit, circling the earth 15 times daily covering latitudes from 82°S to 82°N. Unlike in a previous study[12] we use here the most recent MLS version 5 data of HCl and ozone[36]. These data are used for model initialisation and also for comparison with the simulation results. In the lower stratosphere the vertical resolution is about 3 km and the accuracy of HCl observations is about 0.2 ppbv. The accuracy of ozone observations in the lower stratosphere is about 8%. Unfortunately, the HOCl observations by MLS which would be very interesting for this study are reported to be of sufficient quality only above 10 hPa. We also use MLS ClO data with a systematic uncertainty of 0.25 ppbv above 100 hPa. However in the dark cold polar vortex core, the active chlorine typically resides in chlorine peroxide Cl_2O_2. We therefore show only ClO data within sunlight for solar zenith angles less than 92°.

MIPAS version 8 data

In addition to MLS, we also use $ClONO_2$ measurements from the Michelson Interferometer for Passive Atmospheric Sounding (MIPAS) on Envisat. MIPAS operated between 2002 and 2012 and observed in limb geometry on about 15 orbits per day spanning the latitude range from 87°S to 89°N. In particular, we use $ClONO_2$ mixing ratios employing the retrieval version 8 by the KIT Institute of Meteorology and Climate Research (IMK) in cooperation with the Instituto de Astrofísica de Andalucía (IAA), which are supposed to be the final set (Gabriele Stiller, personal communication, 2025). The used vertical observations modes are labelled V8R_CLONO2_261 and V8R_CLONO2_561. The vertical resolution in the lower stratosphere is about 3-4 km and the accuracy of the $ClONO_2$ observations, derived from correlative measurements, is about 0.05 ppbv[37]. It is difficult to retrieve gas-phase mixing ratios from the infrared spectra in the presence of PSCs due to optical interference. For the frequently occurring optically thick PSCs, a retrieval of gas-phase mixing ratios from MIPAS spectra is likely impossible. Therefore, data gaps due to PSCs are often present in the cold Antarctic stratosphere.

ACE-FTS version 5.2 data

The Atmospheric Chemistry Experiment – Fourier Transform Spectrometer (ACE-FTS) on the SCISAT satellite is a Fourier transform spectrometer with high spectral resolution (0.02 cm^{-1}) operating from a wavelength of 2.2 to 13.3 μm employing a Michelson interferometer[38]. Since 2004, it has observed around 30 profiles per day in solar occultation with the majority of the measurements in high latitudes. Unlike the limb scanning geometry, the coverage of the solar occultation method provides observations at specific latitudes only. The vertical resolution is about 3-4 km. Here we present version 5.2 data for HOCl., which is presently a non-validated research product[24].

Data availability

The satellite data from MLS, MIPAS, and ACE-FTS are publicly available upon registration https://acdisc.gesdisc.eosdis.nasa.gov/data/Aura_MLS_Level2, https://imk-asf-mipas.imk.kit.edu, https://databace.scisat.ca/level2. Data from the presented CLaMS simulations are available by https://doi.org/10.26165/JUELICH-DATA/DNGQOQ and on the SDL Climate Science Data Repository under https://datapub.fz-juelich.de/slcs/clams/polar_hcl_depletion.

Code availability

The CLaMS model code can be downloaded from https://jugit.fz-juelich.de/clams/clams-git.git.

Received: 28 January 2025; Accepted: 18 June 2025;
Published online: 28 June 2025

References

1. Farman, J. C., Gardiner, B. G. & Shanklin, J. D. Large losses of total ozone in Antarctica reveal seasonal ClO_x/NO_x interaction. *Nature* **315**, 207–210 (1985).
2. Stolarski, R. S. et al. Nimbus 7 satellite measurements of the springtime Antarctic ozone decrease. *Nature* **322**, 808–811 (1986).
3. Molina, M. J. & Rowland, F. S. Stratospheric sink for chlorofluoromethanes: chlorine atom-catalysed destruction of ozone. *Nature* **249**, 810–812 (1974).
4. Solomon, S., Garcia, R. R., Rowland, F. S. & Wuebbles, D. J. On the depletion of Antarctic ozone. *Nature* **321**, 755–758 (1986).
5. Crutzen, P. J. & Arnold, F. Nitric acid cloud formation in the cold Antarctic stratosphere: A major cause for the springtime 'ozone hole'. *Nature* **342**, 651–655 (1986).
6. Molina, L. T. & Molina, M. J. Production of Cl_2O_2 from the self-reaction of the ClO radical. *J. Phys. Chem.* **91**, 433–436 (1987).
7. Anderson, J. G., Brune, W. H. & Proffitt, M. H. Ozone destruction by chlorine radicals within the antarctic vortex: The spatial and temporal evolution of ClO-O_3 anticorrelation based on in situ ER-2 data. *J. Geophys. Res.* **94**, 11465–11479 (1989).
8. Solomon, S. Stratospheric ozone depletion: A review of concepts and history. *Rev. Geophys.* **37**, 275–316 (1999).
9. Brakebusch, M. et al. Evaluation of Whole Atmosphere Community Climate Model simulations of ozone during Arctic winter 2004-2005. *J. Geophys. Res.* **118**, 2673–2688 (2013).
10. Solomon, S., Kinnison, D., Bandoro, J. & Garcia, R. Simulation of polar ozone depletion: An update. *J. Geophys. Res.* **120**, 7958–7974 (2015).
11. Wohltmann, I., Lehmann, R. & Rex, M. A quantitative analysis of the reactions involved in stratospheric ozone depletion in the polar vortex core. *Atmos. Chem. Phys.* **17**, 10535–10563 (2017).
12. Grooß, J.-U. et al. On the discrepancy of HCl processing in the core of the wintertime polar vortices. *Atmos. Chem. Phys*. **18**, 8647–8666 (2018).
13. Wohltmann, I. et al. Chemical evolution of the exceptional arctic stratospheric winter 2019/2020 compared to previous arctic and antarctic winters. *J. Geophys. Res. A* **126**, e2020JD034356 (2021).
14. DeHaan, D., Floisand, I. & Stordal, F. Modeling studies of the effects of the heterogeneous reaction ClOOCl+HCl → Cl_2+HOOCl on stratospheric chlorine activation and ozone depletion. *J. Geophys. Res.* **102**, 1251–1258 (1997).
15. DeHaan, D. & Birks, J. Heterogeneous reactions of chlorine peroxide with halide ions. *J. Phys. Chem. A* **101**, 8026–8034 (1997).
16. Warneck, P. Chlorine compounds in stratosphere - HOCl, HOOCl, and ClOO. *Zeitschrift fur Naturforschung Section A-A, J. Phys. Sci.* **32**, 1254–1262 (1977).
17. Burkholder, J. B. et al. *Evaluation No. 19, JPL Publication 19-5*. Chemical Kinetics and Photochemical Data for Use in Atmospheric Studies (Jet Propulsion Laboratory, Pasadena, USA, 2020). http://jpldataeval.jpl.nasa.gov.
18. Carslaw, K. S., Clegg, S. L. & Brimblecombe, P. A thermodynamic model of the system HCl-HNO_3-H_2SO_4-H_2O, including solubilities of HBr, from 328 K to < 200 K. *J. Phys. Chem.* **99**, 11557–11574 (1995).

19. Shi, Q., Jayne, J. T., Kolb, C. E., Worsnop, D. R. & Davidovits, P. Kinetic model for reaction of $ClONO_2$ with H_2O and HCl and HOCl with HCl in sulfuric acid solutions. *J. Geophys. Res.* **106**, 24259–24274 (2001).
20. Yoshinobu, T., Akai, N., Kawai, A. & Shibuya, K. Neon matrix-isolation infrared spectrum of HOOCl measured upon the VUV-light irradiation of an HCl/O_2 mixture. *Chem. Phys. Lett.* **477**, 70–74 (2009).
21. Xu, Z. F. & Lin, M. C. Computational Studies on Metathetical and Redox Processes of HOCl in Gas Phase. III. Its Self-Reaction and Interactions with HNO_x (x=1-3). *J. Phys. Chem. A* **114**, 5320–5326 (2010).
22. Lary, D. J., Chipperfield, M. P., Pyle, J. A., Norton, W. A. & Riishøjgaard, L. P. Three-dimensional tracer initialization and general diagnostics using equivalent PV latitude-potential-temperature coordinates. *Q. J. R. Meteorol. Soc.* **121**, 187–210 (1995).
23. Grooß, J.-U., Brautzsch, K., Pommrich, R., Solomon, S. & Müller, R. Stratospheric ozone chemistry in the Antarctic: What controls the lowest values that can be reached and their recovery? *Atmos. Chem. Phys.* **11**, 12217–12226 (2011).
24. Bernath, P. F., Dodandodage, R., Boone, C. D. & Crouse, J. HOCl retrievals from the Atmospheric Chemistry Experiment. *J. Quant. Spectr. Radiat. Transfer* **264** https://doi.org/10.1016/j.jqsrt.2021.107559 (2021).
25. von Clarmann, T. et al. The MIPAS HOCl climatology. *Atmos. Chem. Phys.* **12**, 1965–1977 (2012).
26. Solomon, S. et al. Emergence of healing in the Antarctic ozone layer. *Science* **353**, 269–274 (2016).
27. McKenna, D. S. et al. A new Chemical Lagrangian Model of the Stratosphere (CLaMS): 1. Formulation of advection and mixing. *J. Geophys. Res.* **107**, 4309 (2002).
28. McKenna, D. S. et al. A new Chemical Lagrangian Model of the Stratosphere (CLaMS): 2. Formulation of chemistry scheme and initialization. *J. Geophys. Res.* **107**, 4256 (2002).
29. Grooß, J.-U. et al. Nitric acid trihydrate nucleation and denitrification in the Arctic stratosphere. *Atmos. Chem. Phys.* **14**, 1055–1073 (2014).
30. Konopka, P. et al. Mixing and ozone loss in the 1999-2000 Arctic vortex: Simulations with the 3-dimensional Chemical Lagrangian Model of the Stratosphere (CLaMS). *J. Geophys. Res*.**109** https://doi.org/10.1029/2003JD003792 (2004).
31. Pommrich, R. et al. Tropical troposphere to stratosphere transport of carbon monoxide and long-lived trace species in the Chemical Lagrangian Model of the Stratosphere (CLaMS). *Geosci. Model Dev.* **7**, 2895–2916 (2014).
32. Tritscher, I. et al. Lagrangian simulation of ice particles and resulting dehydration in the polar winter stratosphere. *Atmos. Chem. Phys.* **19**, 543–563 (2019).
33. Hersbach, H. et al. The ERA5 global reanalysis. *Q. J. R. Meteorol. Soc.* **146**, 1999–2049 (2020).
34. Ploeger, F. et al. The stratospheric Brewer–Dobson circulation inferred from age of air in the ERA5 reanalysis. *Atmos. Chem. Phys.* **21**, 8393–8412 (2021).
35. Froidevaux, L. et al. Validation of Aura Microwave Limb Sounder HCl measurements. *J. Geophys. Res.* **113**, 1–23 (2008).
36. Livesey, N. J. et al. Version 4.2x level 2 and 3 data quality and description document. *JPL D-33509 Rev. E* https://mls.jpl.nasa.gov/data/v4-2_data_quality_document.pdf (2020).
37. Höpfner, M. et al. Validation of MIPAS $ClONO_2$ measurements. *Atmos. Chem. Phys.* **7**, 257–281 (2007).
38. Bernath, P. F. et al. Atmospheric Chemistry Experiment (ACE) Mission overview. *Geophys. Res. Lett*. **32** https://doi.org/10.1029/2005GL022386 (2005).

Acknowledgements

The authors would like to gratefully acknowledge the computing time for the CLaMS simulations granted on the supercomputer JUWELS at Jülich Supercomputing Centre (JSC) within the Earth System Modelling (ESM) under the project ID CLaMS-ESM. We also thank the European Centre for Medium-Range Weather Forecasts (ECMWF) for providing the ERA5 reanalyses. We thank the Aura-MLS team, the Envisat-MIPAS team, and the ACE-FTS team for the enormous work providing their high quality data sets. We finally thank Ingo Wohltmann and two anonymous reviewers for their valuable and constructive comments on the submitted manuscript.

Author contributions

J.U.G. designed the study and performed the CLaMS simulations. R.M., J.N.C., and M.I.H. discussed the chemistry and also worked on the manuscript.

Funding

Open Access funding enabled and organized by Projekt DEAL.

Competing interests

The authors declare no competing interests.

Additional information

Supplementary information The online version contains supplementary material available at https://doi.org/10.1038/s43247-025-02499-4.

Correspondence and requests for materials should be addressed to Jens-Uwe Grooß.

Peer review information *Communications Earth & Environment* thanks Ingo Wohltmann and the other, anonymous, reviewers for their contribution to the peer review of this work. Primary Handling Editors: Keiichiro Hara and Alice Drinkwater. A peer review file is available